RSC Advances

This article can be cited before page numbers have been issued, to do this please use: L. Li, B. Lu, Q. Fan, L. L. Wei, J. Wu, J. Hou, X. Guo and Z. Liu, *RSC Adv.*, 2016, DOI: 10.1039/C6RA01504B.

ROYAL SOCIETY OF CHEMISTRY

www.rsc.org/advances

View Article Online
DOI: 10.1039/C6RA01504B

Journal Name

ARTICLE

Synthesis and pH-responsive self-assembly behavior of a fluorescent amphiphilic triblock copolymer mPEG-*b*-PCL-*b*-PDMAEMA-*g*-PC for the controlled intracellular delivery of doxorubicin

Received 00th January 20xx,
Accepted 00th January 20xx

DOI: 10.1039/x0xx00000x
www.rsc.org/

Lei Li[a], Beibei Lu[a], Qikui Fan[b], Lulu Wei[a], Jianning Wu[a], Jun Hou[d], Xuhong Guo[a, c], Zhiyong Liu[a*]

In this work, a well-defined pH-responsive methoxy poly(ethylene glycol-block-poly(ε-caprolactone)-block-poly[2-(dimethylamino) ethyl methacrylate]-*g*-7-propinyloxy coumarin triblock amphiphilic copolymer (mPEG-*b*-PCL-*b*-PDMAEMA-*g*-PC) were synthesized by combination of atom transfer radical polymerization (ATRP), ring opening polymerization (ROP) and click chemistry. The chemical structures and compositions of these copolymers were characterized by Fourier transform infrared spectroscopy (FT-IR), proton nuclear magnetic resonance (^{1}H NMR). The molecular weights of copolymers were obtained by ^{1}H NMR spectra and gel permeation chromatography (GPC) measurements. Subsequently, polymers could self-assemble into micelles which were investigated by dynamic light scattering (DLS), transmission electron microscopy (TEM), and fluorescence spectra. The pH-responsive self-assembly behavior of these triblock copolymers in water were investigated at different pH value of 5 and 7.4 for controlled doxorubicin release, which were indicated that the release rate of DOX could be effectively controlled by altering pH, and sealed DOX in neutral surroundings and triggered DOX release in acidic surroundings. CCK-8 assays and confocal laser scanning microscopy (CLSM) against HeLa cells indicated that micelles had no associated cytotoxicity, possessed good biodegradability and biocompatibility, identified the location of the DOX in HeLa cells. While DOX-loaded micelles possessed high cytotoxicity to HeLa cells and exhibited inhibition of the proliferation of HeLa cells. Moreover, these flexible micelles with an on-off switched drug release may offer a promising pattern to deliver a wide variety of hydrophobic payloads to tumor cells for cancer therapy.

1. Introduction

Currently, polymeric micelles as promising nanosized antitumor drug carriers are being extensively studied,[1-3] due to their unique properties and structures, such as nanoscale size, core-shell structure, relatively high stability and prolonged circulation in the blood.[4, 5] The ability of amphiphilic block copolymers to self-assemble in selective solvents have been studied widely.[6-8] And much scientific effort have been directed toward engineering 'smart' materials that are able to respond to change such as variations in temperature,[9-11] pH,[12, 13] or light in their environment.[14, 15] Moreover, some stimuli-responsive polymers can make micelles responsive to pH value. In contrast to other pH-sensitive chemotherapeutics delivery system, micelles are spotlighted for the following advantages: (i) high circulation half-life via avoiding non-selective uptake by the reticuloendothelial system (RES), (ii) enhanced solvent power to hydrophobic anticancer drugs, (iii) utilize the enhanced permeability and retention (EPR) effect for passive targeting.[16-19] For example, cancer tissue is also reported to be acidic extracellularly.[20-22] Polymeric micelles offer many unique advantages, such as passive accumulation in tumors, prolong circulation time in blood and the enhanced uptake by tumors.[23-25] In particular, micelles form from block copolymer consisting of poly(ethylene glycol) (PEG) and poly(ε-caprolactone) (PCL) have drawn considerable interests.[26, 27] The PEG with excellent biocompatibility forms the hydrophilic corona in micelles, thereby it can reduce nonspecific adhesion of polymeric micelles surfaces to blood components. PCL, a hydrophobic polymer approved by the FDA for biomedical applications, is biocompatible, biodegradable, and highly

[a]College of Chemistry and Chemical Engineering, Shihezi University/Key Laboratory for Chemical Materials of Xinjiang Uygur Autonomous Region/Engineering Center for Chemical Materials of Xinjiang Bingtuan, Shihezi University, Xinjiang, Shihezi 832003, China.
[b]Center for Materials Chemistry Frontier Institute of Science and Technology Xi'an Jiaotong University Xi'an, Shaanxi 710054, P. R. China.
[c]State Key Laboratory of Chemical Engineering, East China University of Science and Technology, Shanghai 200237, P. R. China.
[d]Department of immunology, Shihezi University School of Medicine/Department of Pathology and Key Laboratories for Xinjiang Endemic and Ethnic Diseases, Shihezi University School of Medicine, Xinjiang 832003, China
[·]DOI: 10.1039/x0xx00000x
*Correspondence to: Zhiyong Liu (E-mail: lzyongclin@sina.com)

View Article Online
DOI: 10.1039/C6RA01504B

permeable to drugs and PCL serves as hydrophobic core in the micelles, which can be used to load water-insoluble drugs.[22, 26, 28, 29] Poly(2-(N, N-dimethylamino)ethyl methacrylate) (PDMAEMA) is a weak base with a p*K*a at about 7. Under the p*K*a, PDMAEMA is hydrophilic as its amine groups are protonated. Above its p*K*a, PDMAEMA is hydrophobic as its amine groups are deprotonated.[30-33] The self-assembly of amphiphilic block copolymers usually requires that copolymers have well-defined structures and narrow polydispersities, whcih were usually reached by using the "living"/controlled polymerization methods, such as atom-transfer radical polymerization (ATRP),[12, 34] and ring-opening polymerization (ROP),[35] and reversible addition-fragmentation chain transfer polymerization (RAFT).[36, 37] Despite the versatility of CRP techniques, it is still a challenge to find feasible means to introduce functional groups onto polymer chains. These functional polymers, for example, fluorescent groups labeled polymers, biofunctionalized polymers and drug containing polymers, which could find wide applications in chemistry, materials science and biomedical science fields.[38-40]Moreover, a fluorescent coumarin unit could be labeled in vivo in order to detect DOX-loaded micelles. "Click" chemistry is a good choice to synthesize well-defined functional polymers. Chen *et al*[41, 42] synthesized poly(vinyl acetate) with fluorescence via a combination of RAFT/MADIX and "click" chemistry. Wang *et al*[43] prepared amphiphilic centipede-like brush copolymers with PCL and poly(ethyl ethylene phosphate) side segments via combination of ROP and click chemistry by one-pot syntheses strategy. Ivonne L *et al*[44] synthesized PDMAEMA-b-PCL-b-PDMAEMA with different composition via ATRP. The encapsulation ability of AmB depend on micelle dynamics and the length of the hydrophilic segment. Mao *et al*[34] synthesized PLLA-b-PDMAEMA copolymers via ROP and ATRP. Zhu *et al*[45] demonstrated that compared to stably shielded polyplexes of PDMAEMA-PEG-PDMAEMA analogue, reversibly shielded DNA polyplexesbased on low molecular weight bioreducible, PDMAEMA-SS-PEG-SS-PDMAEMA triblock copolymers have excellent colloidal stability under physiological salt conditions. Zhu *et al*[27] prepared PEG_{45}-b-PBO_9-b-PCL_{61} triblock and PEG_{45}-b-PCL_{62} diblock copolymers for comparative studies of micelle formation and relative stability in acidic media. You *et al*[46] prepared two types of fluorescent PDI-cored star polyelectrolytes, and unimolecular fluorescent micelles with a perylenediimide core were sensitive to change in pH values. Thomas K *et al*[47] synthesized a set of PEG-PCL-lPEI triblock copolymers, with decreasing hydrophilic/hydrophobic ratio a transition from partly water-soluble micelle-like assemblies to mainly water-insoluble particle-like precipitates was observed. Dong *et al*[48] synthesized PDMAEMA-g-PEG cationic hydrogel nanoparticles by distillation-dispersion copolymerization of methoxy mPEG and DMAEMA. It was found that the PDMAEMA-g-PEG nanoparticles performed pH, ionic strength, and thermosensitivity in water swelling behavior. Ni *et al*[49] prepared a series of well-defined amphiphilic triblock copolymers mPEG-*b*-PCL-*b*-PDMAEMA by a combination of ROP and ATRP, which could self-assemble into micelles or vesicles in PBS buffer solution, depending on the length of PDMA in the copolymer. Agarose gel retardation assays demonstrated that these cationic nanoparticles can effectively condense plasmid DNA. Deng *et al*[50] studied mPEG-*b*-PCL-*b*-PDMAEMA nanoparticles as the codelivery vector of hydrophobic drug and pDNA. Chen *et al*[3] synthesized a well-defined amphiphilic PCL-*b*-[PGMA-*g*-PC]-*b*-P(PEGMA) with fluorescence units through ROP, RAFT and click chemistry, and micelles were used as a nano-reservoir for controlled release of DOX for bladder cancer therapy. Xu *et al*[51] developed pH-sensitive PMs self-assembled from amphiphilic poly(ethylene glycol)-copoly(n-butyl methacrylate-ran-methacrylic acid) for DOX release, simultaneously modifying micellar shell with folate to improve the efficiency of cellular uptake by tumor cells.

In this study, we synthesized a well-defined pH-responsive mPEG-*b*-PCL-*b*-PDMAEMA-*g*-PC with fluorescence units via ROP, ATRP and click chemistry with mPEG-Br as macroinitiator, ε-CL and DMAEMA as monomers. Incorporation of a block with fluorescence units as a End-capping group in the shell displayed fluorescent property as DOX carriers in vitro. The self-assembly and pH responsive properties of the copolymer in water were investigated. The release investigation of DOX from micelles indicated that the release rate of the drug could be effectively controlled by altering the pH value. Meanwhile, the cellular uptake and cytotoxicity test to HeLa cells were performed.

2. Experimental

2.1. Materials

mPEG (Alfa Aesar, M_n = 1900 g/mol), ε-CL (sigma-Aldrich) was distilled under reduced pressure after being treated with CaH_2. Tin(II)ethylhexanoate ($Sn(Oct)_2$, Sigma), 2-Bromoisobutyryl bromide (BIBB, Aldrich), N, N, N', N, 'N''-pentamethyldiethylenetriamine (PMDETA) were purchased from Sigma-aldrich. Copper (I) chloride (99.999 %, Alfa Aesar) were used without further purification. Doxorubicin hydrochloride (DOX·HCl) was purchased from Beijing Huafeng United Technology Co. Ltd. 2-(Dimethylamino)ethyl methacrylate (DMAEMA 98%, Aldrich) was filtered over aluminum oxide to remove the inhibitor (MEHQ) before being polymerized. Tetrahydrofuran (THF) was refluxed over sodium and distilled twice before use. Dimethylformamide (DMF) and triethylamine (TEA) were dried by refluxing over CaH_2 and distilled before use. 7-hydroxy coumarin, propargyl bromide and sodium azide were purchased from Aladdin Reagent Company and used without further purification. Enhanced Cell Counting Kit-8 (CCK-8, Shanghai, Beyotime Biotechnology). Copper (I) chloride (99.999%, Alfa Aesar) were used without further purification. HeLa cells (Institute of cells, CAS, Shanghai) were used as received. Dulbecco's modified eagle medium (DMEM), fetal bovine serum (FBS), pancreatic enzymes were obtained from biological industries. 4% Paraformaldehyde, 4', 6-Diamidino-2-phenylindole (DAPI) and Triton X-100 were purchased from Solarbio.

2. 2 Characterization

^{1}H NMR data were obtained by Nuclear Magnetic Resonance Spectroscopy (NMR) using a BrukerDMX-500 NMR spectrometer with $CDCl_3$ as solvent. Fourier Transform Infrared Spectroscopy (FT-IR) analysis was measured by IR-Affinity-1 Model spectrophotometer using KBr pellets. The molecular weight and molecular weight distribution of copolymers were measured by gel permeation chromatography (GPC) using a Viscotek TDA 302 gel permeation chromatograph and THF was used as eluent. X-ray photoelectron spectroscopy (XPS) was performed using an Axis Ultra spectrometer with a monochromatized Al-Kα X-ray as

View Article Online
DOI: 10.1039/C6RA01504B

excitation source (225 W). The fluorescence spectra were measured by a Hitachi F-2500 fluorescence spectrophotometer at an excitation wavelength of 300 nm. Dynamic light scattering (DLS) measurements were performed by a BECKMAN COULTER Delasa Nano C particle analyzer at a fixed angle of 165°. Before the light scattering measurements, the sample solutions were filtered three times by using Millipore Teflon (Nylon) filters with a pore size of 0.45 µm. All measurements were repeated three times, and the average result were accepted as the final hydrodynamic diameter (D_h) and zeta potential (mV). Samples for transmission electron microscopy (TEM) images were taken on an H-600 transmission electron microscope (Hitachi, Japan) operating at 120 kV. Confocal laser scanning microscopy images (Zeiss CLSM510) images and fluorescence microscope (OLYMPUS U-RFL-T, Japan) were operated at the excitation wavelength of 480 nm.

2. 3 Synthesis of mPEG-*b*-PCL-*b*-PDMAEMA-*g*-PC with fluorescence triblock amphiphilic copolymer

2. 3. 1 Synthesis of mPEG-*b*-PCL diblock copolymer

mPEG-*b*-PCL were synthesized by ROP with different feed ratios ε-CL using $Sn(Oct)_2$ as catalyst. The typical procedure was as follows: mPEG (3.8 g, 2 mmol), ε-CL (6 g, 52.6 mmol), $Sn(Oct)_2$ (0.04 g, 0.1 mmol), and anhydrous toluene (50 mL) were added into a fresh flamed and nitrogen purged round-bottomed flask. The flask was then placed in a thermostatted oil bath at 120°C for 24 h. After the polymerization, the mixture was cooled to room temperature. The product was dissolved in CH_2Cl_2, and precipitated in methanol three times. Finally, the precipitate was dried under vacuum to a constant weight at 35°C. The different degree of polymerization (DP) of PCL were synthesised by ROP in the some way, which were named MP1 and MP2(yield: 90.6% and 95.3%).

2. 3. 2 Synthesis of mPEG-*b*-PCL-Br initiator

Typically, mPEG-*b*-PCL (4 g, 0.2mmol) and triethylamine (3 mL) were first added into a 100 mL dry flask and After 30 mL of anhydrous CH_2Cl_2 was added to dissolve mPEG-*b*-PCL under nitrogen atmosphere.The flask was placed in an ice/water bath. 2.0 mL of 2-bromoisobutyryl bromide was added into the flask dropwise over 1 h, and the reaction mixture was stirred 48 h at 30°C. The precipitate was filtered off. Then, the filtrate was washed three times sequentially with an aqueous solution of sodium bicarbonate and water. The product was further concentrated by a rotary evaporator, and precipitated three times in methanol, and dried under vacuum to a constant weight at 35°C(yield: 72.2% and 74.5%).

2. 3. 3 Synthesis of mPEG-*b*-PCL-*b*-PDMAEMA by ATRP

Synthesis of mPEG-*b*-PCL-*b*-PDMAEMA: a series of mPEG-*b*-PCL-*b*-PDMAEMA were prepared by ATRP of DMAEMA using mPEG-*b*-PCL-Br as initiator and CuBr/PMDETA as catalyst. The reaction procedures are shown in Scheme 1, which named MPD1 and MPD2.

The typical procedure was described below: mPEG-*b*-PCL-Br (0.2 g, 0.03 mmol), DMAEMA (2.0 g, 9.0 mmol), CuBr (0.151 g, 1.0 mmol), PMDETA (0.337 g, 2 mmol), and THF (30 mL). The flask was degassed with three freeze-evacuate-thaw cycles. Then, the polymerization was performed at 65°C for 12 h. After being cooled to room temperature, the reaction flask was open to air, and the crude product was diluted with THF and passed through a neutral alumina column to remove the copper catalysts. Finally it was precipitated thrice into cold hexane, and dried under vacuum to a constant weight at 40°C(yield: 50.6% and 52.3%).

2. 3. 4 mPEG-*b*-PCL-*b*-PDMAEMA with sodium azide

mPEG-*b*-PCL-*b*-PDMAEMA (1.5 g, 0.2 mmol) was dissolved in DMF (15 mL). Sodium azide (0.225 g, 3.46 mmol) was added to this solution, and the mixture was stirred at 65°C for 48 h. The final reaction solution was diluted with DMF and purified by dialysis against water to remove any traces of salts and unreacted reactants using a membrane with molecular weight cutoff of 7000 Da. The azide-containing polymers were collected by freeze-drying.

2. 3. 5 Synthesis of 7-propinyloxy coumarin (PC)

The synthesis procedure was carried out according to the reported mehods.[3, 42] A mixture of 7-hydroxy coumarin (1.62 g, 10 mmol) in acetone (25 mL), K_2CO_3 (1.38 g, 10 mmol), KI (0.083 g, 0.5 mmol) and propargyl bromide (1.2 mL, 15 mmol) was added to a flask, and the mixture was stirred 24 h at 80°C. Then the reaction mixture was cooled to room temperature and extracted with CH_2Cl_2. The combined organic extracts were washed with water, dried over anhydrous $MgSO_4$ and evaporated to afford a crude product, which was purified by recrystallization from anhydrous ethanol to give a white solid (77.8% yield).

2. 3. 6 Synthesis of mPEG-*b*-PCL-*b*-PDMAEMA-*g*-PC by click chemistry

The synthetic pathway was shown in Scheme 1. Azide-containing polymers (1.0 g, 0.057 mmol), CuBr (0.151 g, 1.0 mmol), and PC (80 mg, 0.40 mmol) were purged with nitrogen to remove the dissolved oxygen.), PMDETA (0.337 g, 2 mmol) was added under nitrogen atmosphere. Then the ampoule were sealed and stirred at 60°C in the absence of oxygen for 24 h. The reaction mixture was exposed to air, and the mixture were diluted by DMF, and purified by dialysis against water to remove unreacted reactants using a membrane with molecular weight cutoff of 7000 Da. The resultant polymers mPEG-*b*-PCL-*b*-PDMAEMA-*g*-PC were collected by freeze-drying, which were named MPDP1 and MPDP2(yield: 65.5% and 66.8%).

2. 4 Self-assembly of mPEG-*b*-PCL-*b*-PDMAEMA-*g*-PC in aqueous solution

Samples for UV-vis, DLS and TEM were prepared as follows: mPEG-*b*-PCL-*b*-PDMAEMA-*g*-PC (20 mg) were dissolved in THF (4 mL) and subsequently, deionized water (1 mL) were added dropwise over a period of 30 min under high-speed stirring at room temperature. After 4 h, 8 mL water was added to quench the micellar assembly, subsequently dialyzed (molecular weight cut-off: 3500 Da) against distilled water for 36 h, and micelles with different concentrations could be obtained by diluting with distilled water. During this dialysis process, the hybridized copolymers self-assembled into micelles with PCL cores and mPEG, PDMAEMA shells, which were named MPDP1 and MPDP2.

2. 5 DOX encapsulation and release studies

100 mg of MPDP1/MPDP2 and 10 mg of DOX•HCl was dissolved in DMF (4 mL) separately, and the two solutions were mixed in a vial and stirred for 30 min, a 3-fold excess of TEA were added in order to obtain DOX base. Then the mixture were added dropwise into water (80 mL) using a syringe pump under high-speed stirring. The DOX-containing suspension was then equilibrated under stirring at room temperature for 4 h, followed by thorough dialysis (molecular weight cut-off: 3500 Da) against deionized water for 2 days to remove unloaded

View Article Online
DOI: 10.1039/C6RA01504B

DOX. The obtained DOX-loaded micelles were named D-MPDP1 and D-MPDP2, respectively.

The DOX loading content (DLC) and loading efficiency (DLE) were determined by UV-vis spectrophotometry at 480 nm. To determine the drug loading level, a small portion of DOX-loaded micelles was withdrawn and diluted with DMF to a volume ratio of 9/1 (DMF/H_2O). The amount of DOX encapsulated was quantitatively determined by a UV-vis. The calibration curve used for drug loading characterization were established by the intensity of DOX with different concentrations in DMF/H_2O (9/1, v/v) solutions. The DLC were defined as the weight ratios of entrapped DOX to that of the DOX-loaded micelles. The DLE of DOX was obtained as the weight ratios between DOX incorporated in assembled micelles and that used in fabrication.

$$\text{DLC (wt\%)} = \frac{\text{weight of loaded drug}}{\text{weight of polymer}} \times 100$$

$$\text{DLE (wt\%)} = \frac{\text{weight of loaded drug}}{\text{weight of drug in feed}} \times 100$$

The in vitro DOX release profiles from the MPDP1/MPDP2 assembled micelles were evaluated using buffer solutions with pH values 5 and 7.4 in a dialysis bag (molecular weight cut-off: 3500). The whole bag were placed into 35 mL PBS or acetate buffer and shaken (200 rpm.) at 37°C.

At specified time intervals 4 mL (V_e) samples were taken and an equal volume of fresh buffer added to maintain the total volume. The concentrations of DOX in different samples were analyzed by UV-vis spectrophotometry at 480 nm. The cumulative percent drug release (E_r) was calculated using

Eq. (1). $$E_r(\%) = \frac{V_e \sum_1^{n-1} C_i + V_o C_n}{m_{DOX}} \times 100$$

Where m_{DOX} represented the amount of DOX in the micelle, V_0 was the volume of the release medium (V_0 = 70 mL), C_i represented the concentration of DOX in the i_{th} sample and C_n represented the concentration of DOX in the n_{th} sample. The in vitro release experiments were carried out in triplicate at each pH and the reported results were the average values with standard deviations.

2. 6 Cytotoxicity test

The cytotoxic effects of polymers, free DOX or DOX-loaded mPEG-b-PCL-b-PDMAEMA-g-PC micelles were evaluated against HeLa cells by the standard XTT. To perform cytotoxicity assay, HeLa cells were seeded at a density of 5000 cells per well on a 96-well plate and cultured for 24 h. The samples were prepared at a series of desired concentrations. Every experimental well was treated with the samples for 24 h and others were added with fresh medium as control. After incubation for 24 h, CCK-8 were added into each well to dissolve the formazan by pipetting in and out several times. The absorbance of each well was measured at a test wavelength of 450 nm. The cell viability of samples were calculated as follow:[18, 52, 53]

$$\text{Cell viability (\%)} = \frac{A_{test} - A_{blank}}{A_{control} - A_{blank}} \times 100$$

Where A_{test} and $A_{control}$ represented the intensity determined for cells treated with different samples and for controlling cells, respectively, and A_{blank} was the absorbance of wells without cells.

2. 7. Intracellular release of DOX

Confocal laser scanning microscopy (CLSM) was used to visualize the subcellular localization and intracellular release behavior of DOX-loaded micelles and free DOX for various lengths of time (0.5 h, 4 h and 24 h). First, the HeLa cells were seeded in a glass base dish with a coverslip at a density of 5000 cells and cultured in DMEM supplemented with 10% FBS for 24 h. Then DOX-loaded micelles and free DOX was added, and cells were cultured for 0.5 h, 4 h and 24 h in a humidified 5% CO_2-containing atmosphere. Finally, the location of intracellular fluorescence was validated using a CLSM imaging system (Zeiss CLSM510) at the excitation wavelength of 480 nm.

View Article Online
DOI: 10.1039/C6RA01504B

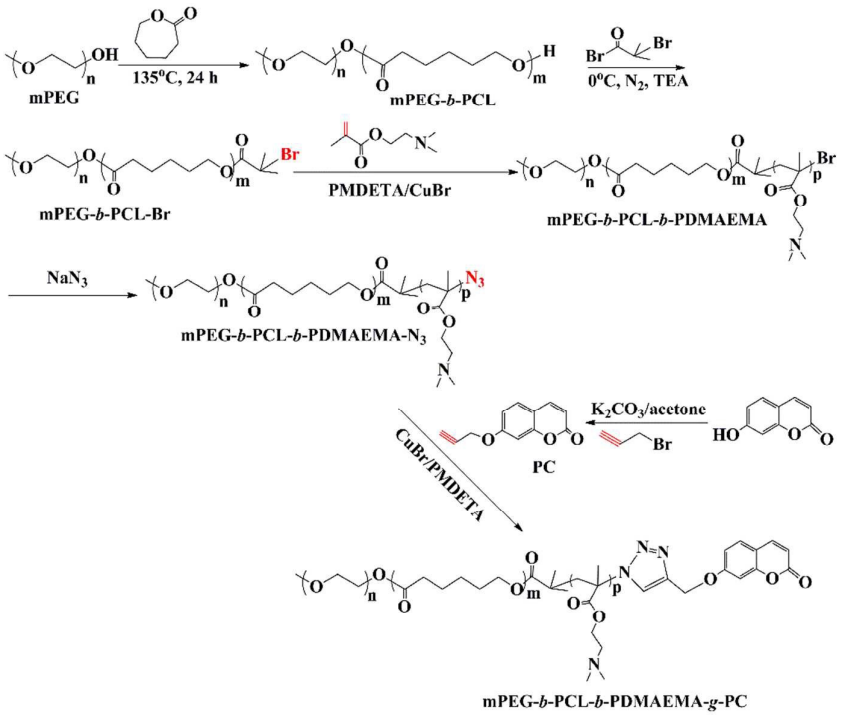

Scheme 1. Synthesis of mPEG-*b*-PCL-*b*-PDMAEMA-*g*-PC with fluorescence triblock amphiphilic copolymer

3. Results and discussion

3. 1 Synthesis and characterization of polymers

The overall experiment was illustrated in Scheme 1. The mPEG-*b*-PCL-*b*-PDMAEMA-*g*-PC were synthesized with different hydrophobic segments by ROP, ATRP and click reaction. The azide-terminated diblock copolymer prepared by a nucleophilic substitution reaction between mPEG-*b*-PCL-*b*-PDMAEMA-Br and NaN_3. Subsequently, the obtained azidofunctionalized copolymer were involved in "click" chemistry with 7-propinyloxy coumarin to prepare fluorescent polymers.

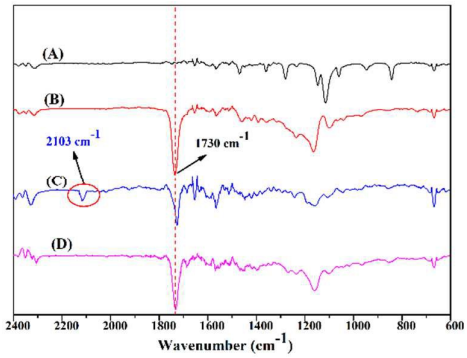

Fig. 1 FT-IR spectra of mPEG (A), mPEG-*b*-PCL (B), mPEG-*b*-PCL-*b*-PDMAEMA-N_3 (C) and mPEG-*b*-PCL-*b*-PDMAEMA-*g*-PC (D).

The FTIR spectra of the mPEG, mPEG-*b*-PCL, mPEG-*b*-PCL-*b*-PDMAEMA-N_3 and mPEG-*b*-PCL-*b*-PDMAEMA-*g*-PC were shown in Fig. 1. The intensive absorption peak at 1730 cm^{-1} of (B), (C) and (D) were assigned to the carbonyl band of PCL in comparison with mPEG (A). mPEG-*b*-PCL was confirmed by ^1H NMR (Fig. 2(B)) and FT-IR (Fig. 1(B)). Moreover, the success of the "click" reaction could also be confirmed from FT-IR spectroscopy from Fig. 1(C). It was clearly observed that the absorption peak at 2103 cm^{-1} attributed to the azide group, and disappeared after the click reaction in Fig.1 (D). All the results demonstrated that the click reaction had been successfully achieved.

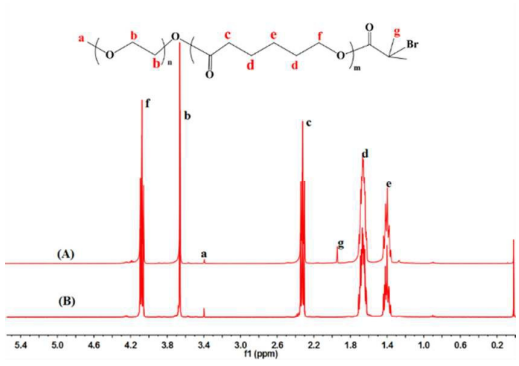

Fig. 2 The ^1H NMR spectra of mPEG-*b*-PCL (B) and mPEG-*b*-PCL-Br (A).

Fig. 2 showed a comparison of ^1H NMR spectra of mPEG-*b*-PCL and mPEG-*b*-PCL-Br with peak assignments in $CDCl_3$. In Fig. 2, the small peak at 3.396 ppm (peak a) and the sharp singlet at 3.650 ppm (peak b) were respectively corresponding to the protons of CH_3O- and -CH_2CH_2O- units of mPEG block, whereas the signals of -CH_2- units of PCL block could be found in peak c, d, e, and f at 2.319 ppm, 1.657 ppm, 1.394 ppm and 4.072 ppm. Moreover, as observed in Fig 2(A), compared with the spectrum of mPEG-*b*-PCL, the ^1H NMR spectrum of mPEG-*b*-PCL-Br displayed new chemical

View Article Online
DOI: 10.1039/C6RA01504B

shifts attributed to the protons of -COC$(CH_3)_2$- at 1.940 ppm (peaks g). The structural characteristics of mPEG-*b*-PCL-*b*-PDMAEMA had been determined by ^{1}H NMR analysis in Fig. 3. We could find the characteristic signals of protons in PDMAEMA block in Fig. 3, the protons of -CH_2N- and -CH_3 of PDMAEMA block were corresponding to the peaks k and i at 2.602 ppm and 0.909 ppm, which could be observed at 2.602 ppm and 0.959 ppm. Furthermore, the overlapped signals at 4.076 ppm, 2.322 ppm, and 1.816 ppm belonged to the protons of -$COOCH_2CH_2$-, -$N(CH_3)_2$ and -$COOCH_2CH_2$- in PDMAEMA block. Synthesis of 7-propinyloxy coumarin (PC) were carried out similar to the procedure described in previous publications in Fig. 4.[3, 42] The resonance at 4.773 ppm was the characteristic signal of the methylene protons of propargyl group, while resonance of the alkenyl proton was observed at 2.602 ppm in Fig. 4.

The obtained azido-functionalized copolymer were subsequently involved in "click" chemistry with 7-propinyloxy coumarin to prepare fluorescence copolymer. The copper (I) and its ligands were reported to be very efficient to catalyze the 1, 3-dipolar cycloaddition of organic azides with terminal alkynes. Herein, CuBr/PMDETA are used as the catalytic system,[54, 55] and DMF as solvent for the 1, 3-dipolar cycloaddition of azido-functionalized copolymer and 7-propinyloxy coumarin. Fig. 5 showed the ^{1}H NMR spectrum recorded for mPEG-*b*-PCL-*b*-PDMAEMA-*g*-PC. The characteristic signals at around 7.680 ppm, 7.407 ppm, 6.963 ppm and 6.315 ppm were assigned to the protons of the coumarin group and the signals of alkenyl group of PC units at 2.602 ppm disappeared completely, which further confirmed the formation of mPEG-*b*-PCL-*b*-PDMAEMA-*g*-PC.

The degrees of polymerization (DP) for the PCL could be calculated about from the integration ratio between the methylene protons (2.32 ppm) in the repeat units and those (3.70 ppm) in the terminal unit based on ^{1}H NMR spectrum.

The molecular weights (M_n, NMR) of MP1, MPD1, MP2 and MPD2 were calculated according to the ^{1}H NMR analysis by the following equations:

$$\frac{A_b}{4\times 43}=\frac{A_c}{2\times N_{CL}} \quad (1)$$

$$\frac{A_b}{4\times 43}=\frac{A_{f+j}}{2\times\left(N_{CL}+N_{DMAEMA}\right)} \quad (2)$$

The number-average molecular weight (M_n) of the copolymer was obtained by the following formula:

M_n of copolymer (MP1 and MP2) = 1900 + 114.14 × N_{CL};

M_n of copolymer (MPD1 and MPD2) = 1900 + 114.14 × N_{CL} + 157.2 × N_{DMAEMA}

Where A_b, A_c and A_{f+j} were the integral values of the peaks b, c and f, j in Fig. 2 respectively; 114.14 was the molecular weight of one repeating unit of the PCL block, 157.2 was the molecular weight of the DMAEMA, and 43 is the polymerization degree of mPEG.

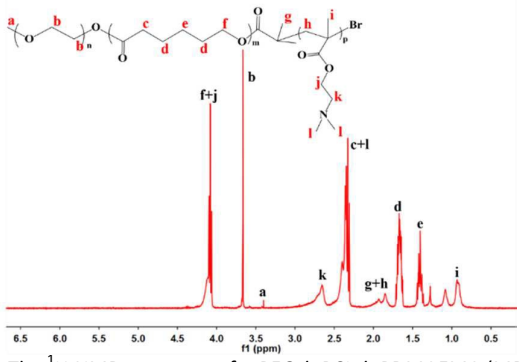

Fig. 3 The ^{1}H NMR spectrum of mPEG-*b*-PCL-*b*-PDMAEMA (MPD2).

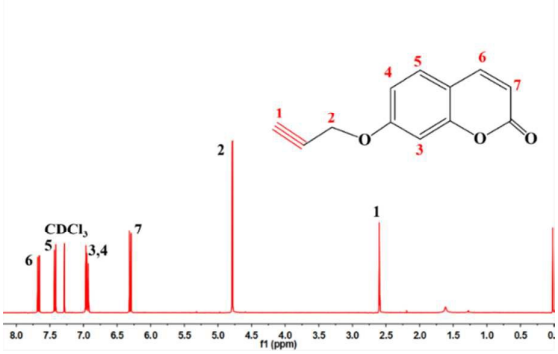

Fig. 4 The ^{1}H NMR spectrum of PC.

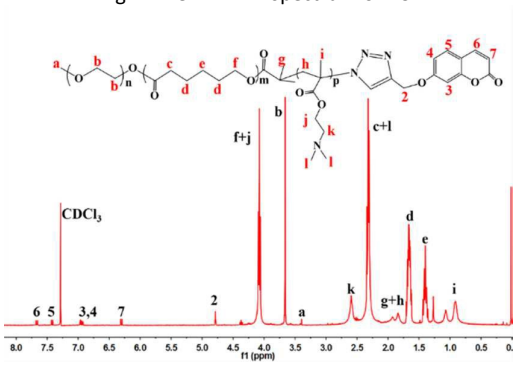

Fig. 5 The ^{1}H NMR spectrum of mPEG-*b*-PCL-*b*-PDMAEMA-*g*-PC

Table 1 Composition of mPEG-*b*-PCL-*b*-PDMAEMA-*g*-PC block copolymers

Samples	$M_{n,Th}$[a]	$M_{n,NMR}$[b]	$M_{n,GPC}$[c]	M_w/M_n[c]
MP1	7942	10035	8990	1.29
MPD1	16320	17940	15980	1.13
MPDP1	——	——	16567	1.15
MP2	10450	13440	12757	1.09
MPD2	18327	19482	23250	1.16
MPDP2	——	——	25258	1.18

[a]Calculated by theory analysis from the feed ratio of monomers to initiator; [b]Calculated from ^{1}H NMR data; [c]Polymerization conditions $[monomer]_0/[mPEG\text{-}b\text{-}PCL\text{-}Br]_0/[CuBr]_0/[PMDETA]_0$=100/1/1/2,

View Article Online
DOI: 10.1039/C6RA01504B

measured by GPC calibrated with PS standards. THF was used as eluent.

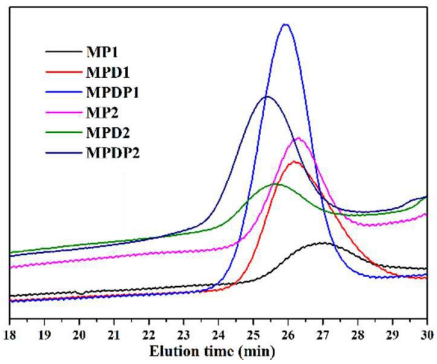

Fig. 6 Evolution of GPC chromatograms of mPEG-*b*-PCL, mPEG-*b*-PCL-*b*-PDMAEMA and mPEG-*b*-PCL-*b*-PDMAEMA-*g*-PC block copolymers.

The GPC traces of MP1, MPD1, MPDP1, MP2, MPD2 and MPDP2 block copolymers were shown in Fig. 6. All the curves of MPD1, MPDP1 and MPD2, MPDP2 shifted to lower elution time compared to that of MP1 and MP2. The detailed information about the molecular weights and PDI of the triblock copolymers were listed in Table 1. The GPC results were almost consistent with the theoretical values and ^{1}H NMR analysis, which were suggested that MPDP block copolymers were synthesized and characterized successfully.

3. 2. Formation and Characterization of the blank and DOX-loaded mPEG-*b*-PCL-*b*-PDMAEMA-*g*-PC (MPDP1 and MPDP2) block copolymers micelles

As an amphiphilic block copolymers, when the concentration were above the critical micelle concentration (CMC), mPEG-*b*-PCL-*b*-PDMAEMA-*g*-PC could self-assemble into micelles in selective solvent. The hydrophilic mPEG and PDMAEMA chains were mainly in the corona of the micelles, whereas the hydrophobic PCL side chains were mainly in the core of the micelles. The hydrophobic of PCL as cores had been extensively used for drug delivery system. DOX was physically incorporated into MPDP1 and MPDP2 polymeric micelles, which were named D-MPDP1 and D-MPDP2. The physico-chemical properties of the blank and DOX-loaded micelles were characterized by DLS analysis, respectively. Hydrodynamic diameter (D_h), polydispersity index (PDI), zeta potentials of the blank and DOX-loaded micelles were summarized in Table 2.

Table 2 Hydrodynamic diameter (D_h), size distributions (PDI) and zeta potentials of blank and DOX-loaded mPEG-*b*-PCL-*b*-PDMAEMA-g-PC micelles.

Micelle	Blank			DOX-load				
	D_h (nm)	PDI	Zeta (mV)	D_h (nm)	PDI	Zeta (mV)	DLC (wt%)	DLE (wt%)
MPDP1	78±1.3	0.280±0.035	24.67±0.32	102±2.5	0.135±0.073	2.50±0.22	4.58	45.8
MPDP2	95±2.2	0.156±0.021	26.05±0.24	115±3.1	0.216±0.035	5.35±0.45	5.43	54.3

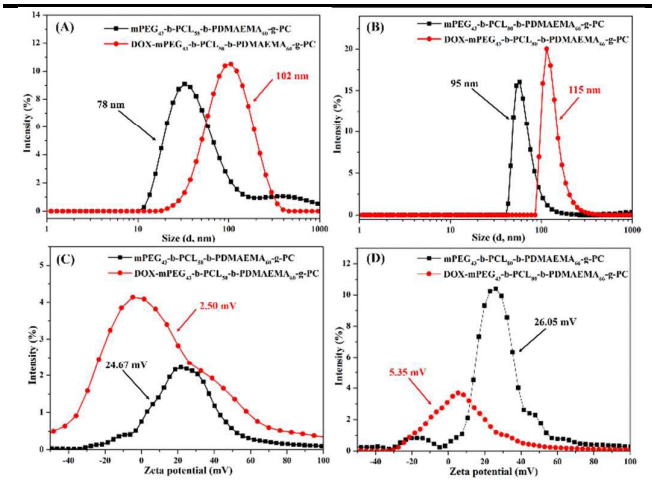

Fig. 7 The particle size distribution curves corresponding to the samples in MPDP1 and D-MPDP1 (A), MPDP2 and D-MPDP2 (B) and zeta potentials of DOX-loaded polymeric micelles in MPDP1 and D-MPDP1 (C), MPDP2 and D-MPDP2 (D).

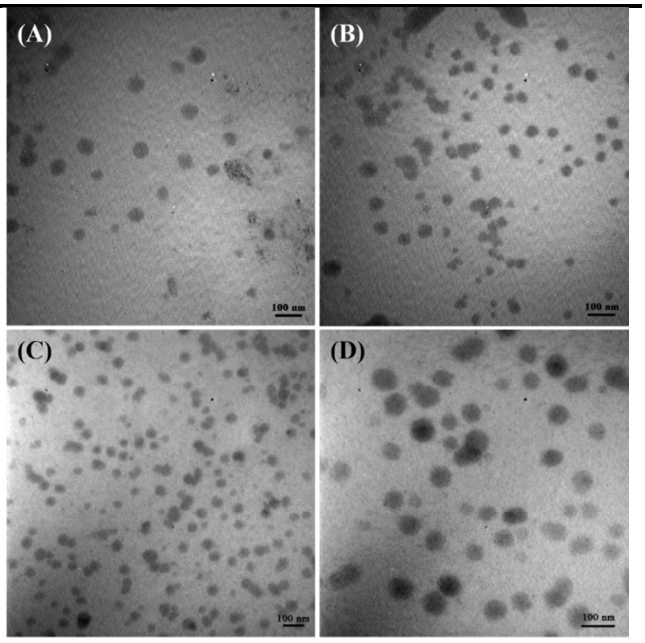

View Article Online
DOI: 10.1039/C6RA01504B

Fig. 8 TEM images of mPEG-*b*-PCL-*b*-PDMAEMA-*g*-PC polymeric micelles (MPDP1 (A, B) and MPDP2 (C, D)).

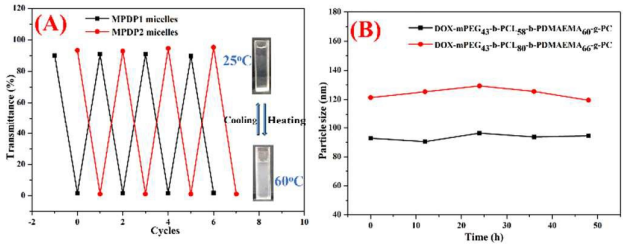

Fig. 9 Plots of transmittance as a function of temperature for mPEG-*b*-PCL-*b*-PDMAEMA-*g*-PC copolymer micelle solution (A), particle size of the mPEG-*b*-PCL-*b*-PDMAEMA-*g*-PC in H_2O at room temperature (B).

As shown in Fig. 7. The D_h, PDI and zeta potential of the micelles were evaluated by DLS and TEM. The combination of TEM and DLS data showed a spherical morphology with the respective average radii around 78 and 95 nm, respectively(Fig. 7, and Table 2). In contrast, D_h were measured by TEM in Fig 8, respectively, the smaller size were probably due to the difference in the two measuring methods. The dehydration of the micellar shell during the TEM samples preparation process may have led to a decrease in the size of the micelles. Further, discrepancies were expected because DLS, reported an intensity-average diameter, whereas TEM reported a number-average diameter. Thus, for a given size distribution of finite polydispersity, TEM images will always undersize relative to DLS data. When DOX was loaded into the polymeric micelles in the core and adsorbed drug on the surface. It could also be found that the zeta potentials of the drug-loaded micelles were lower than those of blank micelles for both of the polymers, resulting from decreased charge density because of larger particle sizes in the Table 2 and Fig. 7. As shown in Fig. 9, a stability assay in terms of transmittance and particle size of mPEG-*b*-PCL-*b*-PDMAEMA-*g*-PC micelles were investigated in water for (A) and (B). The MPDP1 (A) micelles presented reversible transformation of transparency and turbidity during the reversible cooling and heating cycles, when the temperature increases, hydrogen bonding could not be weakened but micelles start to contract because of the decrease in electrostatic repulsion between PDMAEMA chains, indicating that the coronas are hydrophobic to some extent. Obviously, the phase transition of the micelles were reversible, which indicated that the mPEG-*b*-PCL-*b*-PDMAEMA-*g*-PC micelles were stable. As shown in Fig. 9(B), no obvious change of the particle size of the D-MPDP1 and D-MPDP2 micelles during 50 h indicated that the micelles had a well long-term stability without the presence of precipitation and phase separation. The result revealed that the MPDP1 and MPDP2 micelles could offer the protection of drugs from untimely structure disintegration and premature drug release until arriving a disease site.

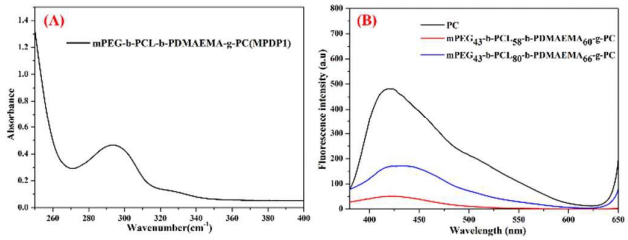

Fig. 10 (a) UV-vis spectrum of MPDP1 micelles and (b) fluorescence spectra of mPEG-*b*-PCL-*b*-PDMAEMA-*g*-PC micelles solution.

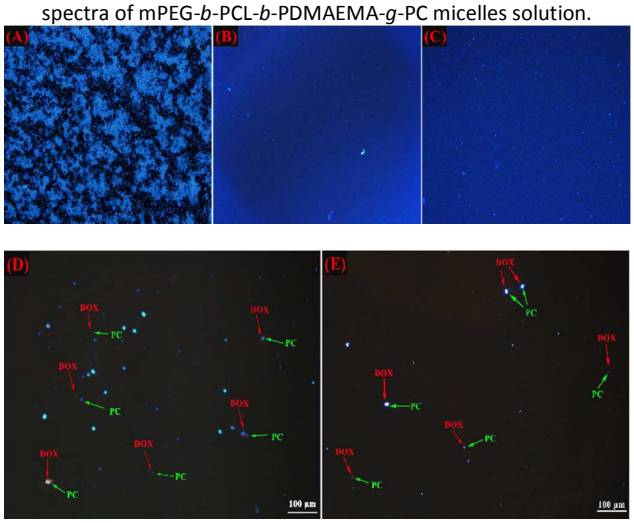

Fig. 11 Fluorescence images of PC (A), MPDP1 (B)， MPDP2 (C)，D-MPDP1 (D) and D-MPDP2 (E) micelles. PC (blue), DOX (red).

The UV-vis spectrum of MPDP1 micelles showed a characteristic UV-vis absorption peak of coumarin moiety at 300 nm in Fig. 10 (A). The fluorescence spectra of mPEG-*b*-PCL-*b*-PDMAEMA-*g*-PC were displayed in Fig. 10(B). It could be observed that the triblock copolymer, obtained by coupling of azide-containing polymers with 7-propinyloxy coumarin, exhibited a strong fluorescence peak at about 425 nm. Fig. 11 showed fluorescence images of PC (A), MPDP1 (B)， MPDP2 (C)，D-MPDP1 (D) and D-MPDP2 (E) micelles. We could see bright blue of PC, MPDP1 and MPDP2 in Fig.11(A, B and C). The DOX-loaded micelles displayed the bright blue fluorescence corresponding to the coumarin dye implying that the fluorescent micelles had been effectively internalized.

3. 3 In vitro release of DOX from micelles

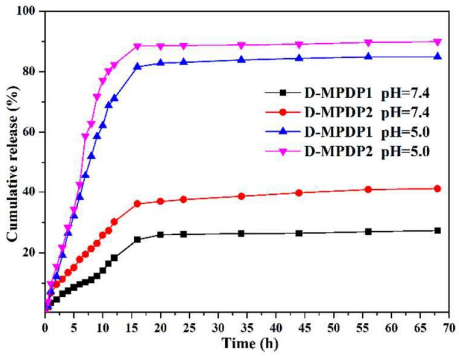

Fig. 12 In vitro release of DOX from various DOX-loaded polymeric micelles at 37 °C under different pH conditions.

As expected, the mPEG-*b*-PCL-*b*-PDMAEMA-*g*-PC micelles exhibited a pH-responsive characteristic. In vitro drug release performances of the micelles were performed under physiological conditions (PBS, pH= 5 and 7.4) at 37°C in Fig. 12. It could be observed that the drug release rates of DOX from micelles were obviously changed by pH values as well as time. With regard to pH of 7.4 at 37°C, the micelles stayed compact and the loaded DOX was released slowly. After 5 h, less than 20% of DOX (8.6% and 15.1% for D-MPDP1 and D-MPDP2, respectively) were released. Even after

View Article Online
DOI: 10.1039/C6RA01504B

24 h, only about 26.1% and 35.1% for D-MPDP1 and D-MPDP2 were released, respectively. In contrast, when the pH was lower at 37°C (pH=5), the drug release were accelerated. After 24 h, the cumulative release were 83.1% and 88.7% for D-MPDP1 and D-MPDP2, respectively. Although the mechanism of drug release from polymeric matrices was very complex and was still not completely understood, it could be simplistically classified as either pure diffusion, erosion controlled release or a combination of the two mechanisms.[56, 57] In this study, the results were due to the swollen drug-loaded micelles, attributing to the protonation of amino groups in PDEAEMA segments at weakly acidic conditions. Furthermore, the accelerated micelles rate might be related to the swollen hydrophobic core, which could cause the drug molecules close to the surface to diffuse into the medium. Meanwhile, the DOX molecules were not only encapsulated inside the micellar core, but also absorbed by the PDMAEMA shell due to the electric action, while only that loaded by hydrophobic effect could be released comparatively fast, so it might spend extended period to achieve complete release. These MPDP1 and MPDP2 micelles were just like on-off switching nanocarriers in release kinetics by changing pH values. Therefore, it were highly interesting for intracellular anti-cancer drug delivery.

3. 4 Cytotoxicity test

Cytotoxic effects of the polymers, free DOX or DOX-loaded micelles in HeLa cells were determined by CCK-8 assay. The cell viability of blank micelles and DOX-loaded micelles against HeLa cells were evaluated. The cell viability of blank micelles were measured after 48 h incubation. The blank micelles with different concentration were nontoxic to HeLa cells and the cell viability were over 95% at all concentrations (12.5~200 μg/mL) tested in Fig. 13, which were indicated that the blank micelles could be used as a delivery system for anticancer agents.

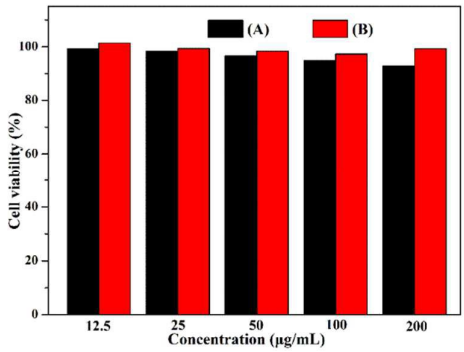

Fig 13 In vitro cell viability of the mPEG-*b*-PCL-*b*-PDMAEMA-*g*-PC micelles. Concentration-dependent cell viability of HeLa cells treated with the MPDP1 (A) and MPDP2 (B) after incubation of 48 h.

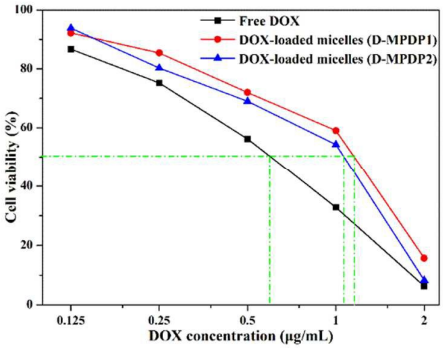

Fig. 14 Cell viability of HeLa cells incubated with free DOX, DOX-loaded micelles (D-MPDP1 and D-MPDP2) for 48 h at different concentrations.

Fig. 14 showed the results of samples treated with free DOX and DOX-loaded micelles for 48 h, respectively. The DOX dosages required for the inhibitory concentration to produce 50% cell death (IC_{50}) were 0.633 μg/mL, 1.208 μg/mL, 1.092 μg/mL for 48 h for free DOX, D-MPDP1 and D-MPDP2 against HeLa cells, this slight difference between two DOX-loaded micelles could be explained that the latter containing more PCL segments, leading to higher drug loading level and more sensitive, respectively. Both of the DOX loaded micelles showed slightly lower cytotoxicity than free DOX due to the time-consuming DOX release from micelles in comparison to free DOX at the same concentration. All of DOX-loaded micelles had a similar capacity of killing tumor cells as free DOX for 48 h, which were indicated that DOX-loaded micelles might not inhibit the ability of killing cells although it slowed down the release of DOX. Moreover, the results revealed that DOX released from the micelles could exploit a potent drug efficacy as free DOX after entry into the HeLa cells. It could produce the desired pharmacological action and minimize the side effect of free DOX.

3. 5 In vitro cellular uptake studies

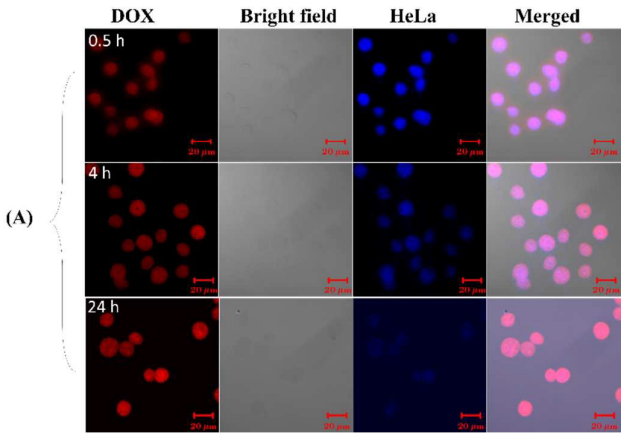

View Article Online
DOI: 10.1039/C6RA01504B

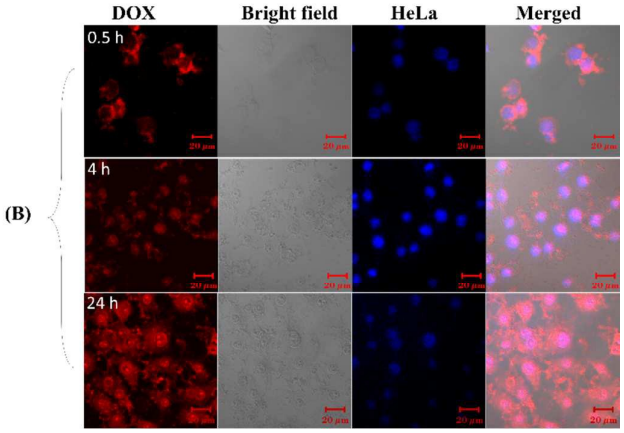

Fig. 15 Confocal laser scanning microscopy images of HeLa cells incubated with (A) free DOX and (B) DOX-loaded (D-MPDP2) for different times. The DOX dosage was 10 μg/mL. For each panel, images from left to right show cell nuclei stained by DOX fluorescence in cells (red), bright field of cells, HeLa (blue), and overlays of the blue and red images. The scale bars are 20 μm in all images.

To evaluate the intracellular uptake efficiency, confocal laser scanning microscopy were used to identify the location of the DOX in HeLa cells. The CLSM of HeLa cells after 0.5, 4 and 24 h of incubation with free DOX and DOX-loaded micelles (D-MPDP2) were presented in Fig. 15. After incubation for 0.5 h, stained with DAPI, the nuclei and cytoplasm of pretreated cells were observed by CLSM. By comparison with the control in Fig. 15(B), the observation revealed that free DOX was slightly accumulated in the cell nuclei of HeLa cells in Fig. 15(A). After incubation for 4 h and 24 h, free DOX was larger accumulated than DOX-loaded micelles (D-MPDP2). While DOX released from D-MPDP2 were mainly located in the cytoplasm, and DOX was released into the cytoplasm and nuclei of cells under acid conditions in lysosomes in Fig. 15(A and B). The result also indicated that free DOX was taken up by diffusion through the cell membrane and the DOX loaded micelles were taken up by the nuclei of cells via the indocytosis process. Moreover, the self-assembled micelles showed a great potential as anti-tumor drug carriers for cancer therapy.

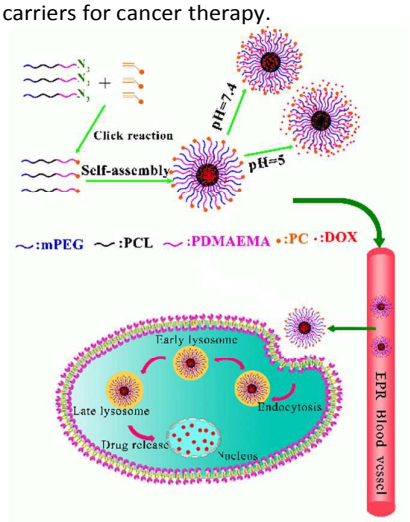

Scheme 2. Illustration of pH-responsive self-assembly of mPEG-*b*-PCL-*b*-PDMAEMA-*g*-PC copolymer for the efficient intracellular release of anti-cancer drugs triggered by the acidic microenvironment inside the tumor tissue.

4. Conclusion

In the current work, we had reported pH-responsive mPEG-*b*-PCL-*b*-PDMAEMA-*g*-PC copolymers by click chemistry, ROP, ATRP with fluorescence units for cancer therapy. The Hydrodynamic diameter, polydispersity index (PDI) and zeta potential of the mPEG-*b*-PCL-*b*-PDMAEMA-*g*-PC micelles were evaluated by DLS and TEM, and the sizes of MPDP1 and MPDP2 micelles with spherical shapes determined by TEM were about 78 nm and 95 nm. These copolymers could markedly improve micellar stability and extend the range of applications of micelles in controlling drug delivery with increasing PCL segments. In addition, DOX-loaded micelles had a fluorescence, which were investigated by fluorescence spectrophotometer and fluorescence microscope in order to label the location of drug in vivo.

The release behaviors of DOX from micelles exhibited pH-responsive in vitro, the DOX loading contents were the higher as the PCL segment increased. And the release of DOX from the micelles were significantly accelerated by decreasing pH from 7.4 to 5.0 at 37°C. After 50 h for D-MPDP2 micelles, the cumulative release were about 88.7% (w/w), which could be provided sustained drug delivery behavior after the DOX-loaded micelles entered into blood circulation by endocytosis. In addition, the cytotoxicity tests revealed that these MPDP micelles possessed good biodegradability and biocompatibility for the HeLa cells and the DOX-loaded micelles showed much higher toxic effect, which were almost similar to free DOX. Moreover, the DOX loaded micelles were taken up by the nuclei of cells via the indocytosis process by CLSM. Furthermore, the applicability of these micelles toward tumor-targeting delivery applications in vivo is highly promising chemotherapy in the future.

Acknowledgements

The authors gratefully acknowledge financial supports from the National Natural Science Foundation of China (21367022) and Bingtuan Innovation Team in Key Areas (2015BD003).

References

1. X. Zhang, C. Wang, S. Fang, J. Sun, C. Li, Y. Hu, *Colloid Polym. Sci.*, 2012, **291,** 789-803.
2. S. Guo, Y. Huang, T. Wei, W. Zhang, W. Wang, D. Lin, X. Zhang, A. Kumar, Q. Du, J. Xing, L. Deng, Z. Liang, P.C. Wang, A. Dong, X.J. Liang, *Biomaterials*, 2011, **32**, 879-889.
3. J. Chen, M. Liu, *RSC Adv.*, 2014, **4**, 9684-9692.
4. C.Y. Chen, T.H. Kim, W.C. Wu, C.M. Huang, H. Wei, C.W. Mount, Y. Tian, S.H. Jang, S.H. Pun, A.K. Jen, *Biomaterials*, 2013, **34**, 4501-4509.
5. J. Gong, M. Chen, Y. Zheng, S. Wang, Y. Wang, *J. Control. Release*, 2012, **159**, 312-323.
6. Y. Lu, K. Park, *Int. J. Pharm.*, 2013, **453**, 198-214.
7. X. Zhao, P. Liu, *ACS Appl. Mater. Inter.*, 2015, **7**, 166-174.
8. H. Liu, K. Miao, G. Zhao, C. Li, Y. Zhao, *Polym. Chem.*, 2014, **5**, 3071-3080.
9. G. Liu, Q. Qiu, Z. An, *Polym. Chem.*,2012, **3**, 504-513.

View Article Online
DOI: 10.1039/C6RA01504B

10. L.A. Fielding, J.A. Lane, M.J. Derry, O.O. Mykhaylyk, S.P. Armes, *J. Am. Chem. Soc*., 2014, **136** 5790-5798.
11. M. Wang, Y. Gao, C. Cao, K. Chen, Y. Wen, D. Fang, L. Li, X. Guo, *Ind. Eng. Chem. Res*., 2014, **53**, 18462-18472.
12. Z.Y. Ma, X. Jia, G.X. Zhang, J.M. Hu, X.L. Zhang, Z.Y. Liu, H.Y. Wang, F. Zhou, *J. Agr. Food Chem*., 2013, **61**, 5474-5482.
13. Z. Wang, B.H. Tan, H. Hussain, C. He, *Colloid Polym*. *Sci.*, 2013, **291**, 1803-1815.
14. Y. Zakrevskyy, M. Richter, S. Zakrevska, N. Lomadze, R. von Klitzing, S. Santer, *Adv. Funct. Mater*., 2012, **22**, 5000-5009.
15. Z. Zhu, E. Senses, P. Akcora, S.A. Sukhishvili, *ACS Nano*, 2012, **6**, 3152-3162.
16. Y. Lv, G. Ding, J. Zhai, Y. Guo, G. Nie, L. Xu, *Colloid Surface B*, 2013, **110**, 411-418.
17 H. Wu, L. Zhu, V.P. Torchilin, *Biomaterials*, 2013, **34** 1213-1222.
18. C. Yu, C. Gao, S. Lü, C. Chen, J. Yang, X. Di, M. Liu, *Colloid Surface B*, 2014, **115**, 331-339.
19. L. Qiu, Z. Li, M. Qiao, M. Long, M. Wang, X. Zhang, C. Tian, D. Chen, *Acta Biomater*., 2014, **10**, 2024-2035.
20. B. Sahoo, K.S. Devi, R. Banerjee, T.K. Maiti, P. Pramanik, D. Dhara, *ACS Appl. Mater. Inter*., 2013, **5**, 3884-3893.
21. F. Hu, K.G. Neoh, E.T. Kang, *Macromol. Rapid. Commun.,* 2009, **30**, 609-614.
22. H. Wang, J. He, M. Zhang, Y. Tao, F. Li, K.C. Tam, P. Ni, *J. Mater. Chem. B*, 2013, **1**, 6596-6607.
23. J. Chen, M. Liu, H. Gong, Y. Huang, C. Chen, *J. Phys. Chem. B*, 2011, **115**, 14947-14955.
24. R. Cheng, F. Feng, F. Meng, C. Deng, J. Feijen, Z. Zhong, *J. Control. Release,* 2011, **152**, 2-12.
25. H. Wei, R.-X. Zhuo, X.-Z. Zhang, *Prog. Polym. Sci*., 2013, **38**, 503-535.
26. T. Endres, M. Zheng, A. Kilic, A. Turowska, M. Beck-Broichsitter, H. Renz, O.M. Merkel, T. Kissel, *Mol. Pharm*., 2014, **11**, 1273-1281.
27. X. Zhu, M. Fryd, B.D. Tran, M.A. Ilies, B.B. Wayland, *Macromolecules*, 2012, **45**, 660-665.
28. L.S. Nair, C.T. Laurencin, *Prog. Polym. Sci*., 2007, **32**, 762-798.
29. N.J. Warren, O.O. Mykhaylyk, D. Mahmood, A.J. Ryan, S.P. Armes, *J. Am. Chem. Soc*., 2014, **136**, 1023-1033.
30. J. Chen, P. Xiao, J. Gu, Y. Huang, J. Zhang, W. Wang, T. Chen, *RSC Adv*., 2014, **4**, 44480-44485.
31. X. Han, X. Zhang, H. Zhu, Q. Yin, H. Liu, Y. Hu, *Langmuir*, 2013, **29**, 1024-1034.
32. T. Ren, X. Lei, W. Yuan, *Mater. Lett*., 2012, **67**, 383-386.
33. A.P. Majewski, U. Stahlschmidt, V. Jerome, R. Freitag, A.H. Muller, H. Schmalz, *Biomacromolecules*, 2013, **14**, 3081-3090.
34. J. Mao, X. Ji, S. Bo, *Macromol. Chem. Phys*., 2011, **212**, 744-752.
35. A.M. Master, M.E. Rodriguez, M.E. Kenney, N.L. Oleinick, A.S. Gupta, *J. Pharm. Sci*., 2010, **99**, 2386-2398.
36. L. Hong, Z. Zhang, W. Zhang, *Ind. Eng. Chem. Res*., 2014, **53**, 10673-10680.
37. J. Chen, M. Liu, C. Gao, S. Lü, X. Zhang, Z. Liu, *RSC Adv.,* 2013, **3**, 15085-15093.
38. C.W. Scales, A.J. Convertine, C.L. McCormick, Biomacromolecules 7 (2006) 1389-1392.
39. C. Li, Y. Zhang, J. Hu, J. Cheng, S. Liu, *Angew. Chem. Int. Edit*., 2010, **122**, 5246-5250.
40. D. Bontempo, K.L. Heredia, B.A. Fish, H.D. Maynard, *J. Am. Chem. Soc*., **2014**, 126, 15372-15373.
41. L.-J. Zhang, B.-T. Dong, F.-S. Du, Z.-C. Li, *Macromolecules* 2012, **45**, 8580-8587.
42. F. Chen, Z. Cheng, J. Zhu, W. Zhang, X. Zhu, *Eur. Polym. J*., 2008, *44*, 1789-1795.
43. Y.-Y. Yuan, Q. Du, Y.-C. Wang, J. Wang, *Macromolecules*, 2010, **43**, 1739-1746.
44. I.L. Diaz, L.D. Perez, *Colloid. Polym. Sci*., 2014, **293**, 913-923.
45. C. Zhu, M. Zheng, F. Meng, F.M. Mickler, N. Ruthardt, X. Zhu, Z. Zhong, *Biomacromolecules*, 2012, **13**, 769-778.
46. S. You, Q. Cai, K. Mullen, W. Yang, kM. Yin, *Chem. Commun*., 2014, **50**, 823-825.
47. T.K. Endres, M. Beck-Broichsitter, O. Samsonova, T. Renette, T.H. Kissel, *Biomaterials*, 2011, **32** (2011) 7721-7731.
48. A. Dong, Y. Zhai, L. Xiao, H. Qi, Q. Tian, L. Deng, R. Guo, *J. Polym. Sci. Pol. Phys*., 2010, **48**, 503-508.
49. W. Zhang, J. He, Z. Liu, P. Ni, X. Zhu, *J. Polym. Sci. Part A: Polym. Chem*., 2010, **48**, 1079-1091.
50. X. Yue, Y. Qiao, N Qiao, S. Guo, J. Xing, L. Deng, J. Xu, A. Dong, *Biomacromolecules*, 2010, **11**, 2306-2312.
51. Z. Xu, M. Guo, H. Yan, K. Liu, *React. Funct. Polym*., 2013, **73**, 564-572.
52. Q. Liu, J. Chen, J. Du, *Biomacromolecules*, 2014, **15**, 3072-3082.
53. M. Zhang, Q. Xiong, J. Chen, Y. Wang, Q. Zhang, *Polym. Chem*., 2013, **4**, 5086-5095.
54. L.Y. Li, W.D. He, J. Li, S.C. Han, X.L. Sun, B.Y. Zhang, *J. Polym. Sci. Pol. Chem*., 2009, **47**, 7066-7077.
55. B.-Y. Zhang, W.-D. He, W.-T. Li, L.-Y. Li, K.-R. Zhang, H. Zhang, *Polymer*, 2010, **51**, 3039-3046.
56. C.R. Young, C. Dietzsch, M. Cerea, T. Farrell, K.A. Fegely, A. Rajabi-Siahboomi, J.W. McGinity, *Int. J. Pharm*., 2005, **301**, 112-120.
57. F. Zhu, Q. Yang, Y. Zhuang, Y. Zhang, Z. Shao, B. Gong, Y.-M. Shen, *Polymer*, 2014, **55**, 2977-2985.

View Article Online
DOI: 10.1039/C6RA01504B

Schematic illustration of pH-responsive self-assembly of mPEG-*b*-PCL-*b*-PDMAEMA-*g*-PC copolymer with a fluorescent coumarin units for controlling the DOX release